ELSEVIER

Journal of Alloys and Compounds 317–318 (2001) 595–602

Journal of ALLOYS AND COMPOUNDS

www.elsevier.com/locate/jallcom

Electrochemical behaviour of Cu–Zr and Cu–Ti glassy alloys

K. Brunelli[a], M. Dabalà[a,*], R. Frattini[b], G. Sandonà[c], I. Calliari[a]

[a]*Dipartimento di Innovazione Meccanica e Gestionale, Università di Padova, Via Marzolo, 9, Padova, 35100 Italy*
[b]*INFM – Dipartimento di Chimica Fisica, Università di Venezia, Dorsoduro 2137, Venice, 30100 Italy*
[c]*Dipartimento di Chimica Fisica, Università di Padova, Via Loredan, 2, Padova, 35100 Italy*

Abstract

Hydrogen evolution is a fundamental reaction for better understanding of electrochemical activity of electrode materials. Amorphous Cu–Zr and Cu–Ti ribbons were produced by melt spinning methods and were characterized by X-ray diffraction, scanning electron microscopy and differential scanning calorimetry. The electrocatalytic efficiency was evaluated on the basis of electrochemical data obtained from cathodic polarization curves carried out in both acid and basic medium at 25°C. The surfaces of amorphous materials were prepared, before electrochemical measurements, by immersion in HF solutions. The results were compared to those obtained on polycrystalline copper and on untreated ribbons. The HF treatment yielded a porous copper structure with a higher roughness factor which had improved electrocatalytic activity compared with that of polycrystalline copper electrode.

Keywords: Amorphous alloys; Hydrogen evolution reaction; Differential scanning calorimetry; Activation surface treatments; Hydrofluoric acid

1. Introduction

Hydrogen is an excellent candidate as an efficient and inexpensive energy carrier. In fact, it is non-polluting, recyclable and available in unlimited quantities. Since hydrogen can be produced by electrolysis of water, improvements in electrode materials to make the technique economically practical, are required. Because amorphous alloys prepared by a rapid quenching from their melts, possess high mechanical strength and good corrosion resistance, as well as a defect-free homogeneous structure, they are attractive as electrode materials for the hydrogen evolution reaction. Moreover, the melt quenching techniques allow the production of metallic composition not available from traditional processes. This is important in electrocatalysis because the Brewer–Engle theory predicts high electrocatalytic activities in the hydrogen electrode reaction for certain combinations of transition metals [1]. Early transition metals, with empty or half-filled d orbitals, alloyed with late groups elements, with internal paired d electrons not available for bonding in the pure metals, can generate electronic structures with higher catalytic activity than either component alone [2]. Also several amorphous alloys, containing Ti and Zr especially, have been investigated with a view to hydrogen storage since they are not pulverized upon adsorption and desorption of hydrogen and, in addition, have an improved amount of hydrogen absorption rate as compared with their crystalline counterparts [3–10]. However the activity for the cathodic hydrogen evolution increases dramatically after an appropriate surface treatment [11]. In fact, the surfaces of melt quenched alloys are covered by thin oxide layers which must be removed by chemical etching. In the case of amorphous Zr and Ti containing alloys, pretreatment with HF significantly enhances the electrocatalytic activity either by removing the surface oxide layers or by increasing the surface areas of the materials [12].

In this work the electrocatalytic activity of amorphous $Cu_{60}Zr_{40}$, $Cu_{40}Ti_{60}$, $Cu_{40}Zr_{60}$, $Cu_{60}Ti_{40}$ alloys in the hydrogen evolution reaction in both acid and alkaline medium, was investigated. The effect of activation treatments in 0.1 and 1 M HF on structure, surface and electrocatalytic activity was reported and discussed.

2. Experimental details

Some 1-mm wide, 30-μm thick $Cu_{60}Zr_{40}$, $Cu_{40}Zr_{60}$, $Cu_{60}Ti_{40}$ and $Cu_{40}Ti_{60}$ ribbons were produced by melt

*Corresponding author. Tel.: +39-049-827-5503; fax: +39-049-827-5500.

E-mail addresses: manolo@ux1.unipd.it (M. Dabalà), frattini@unive.it (R. Frattini).

0925-8388/01/$ – see front matter
PII: S0925-8388(00)01394-3

spinning method in vacuum at a cooling wheel rate of 3000 cm/s.

The structure of the alloys was studied by X-ray diffraction (XRD) measurements. XRD patterns were collected with a Bragg–Brentano powder diffractometer using Cu Kα radiation (λ=1.54178 Å) and a graphite monochromator in the diffracted beam. The crystalline particle size has been determined from the broadening of the diffraction peaks [13]. Phase transformations were followed by a Perkin Elmer DSC7 under flowing nitrogen. The surface of the alloys was investigated by scanning electron microscopy (SEM) with a Cambridge Stereoscan 440 equipped with EDS microbeam.

The amorphous alloys underwent at two different surface activation treatments with immersion in 1 M HF solutions for 30 s or in 0.1 M HF solution for 1 min and rinsed with H_2O.

Electrochemical characterization of the samples was achieved by means of cathodic polarization, with scanning rate of 1 mV/s, in both oxygen free 1 N KOH and 1 N H_2SO_4 at 25°C. For comparison some tests were performed on a polycrystalline Cu electrode having surface area of ~1 cm^2. In this work the electrocatalytic activity was evaluated on the basis of apparent unit area of the electrodes.

3. Results and discussion

Fig. 1 shows the XRD patterns of the as-quenched alloys: the amorphous condition of the materials is revealed. The distance *a* between a large number of pairs of glass constituents representing the smallest distance of approach of the atom, is evaluated by the Ehrenfest relation [14]; the results are summarized in Fig. 2. The parameter *a* decreases more rapidly in Zr-containing alloys as Cu content increases, than in Ti-containing alloys. These results are in agreement with data obtained with both XRD and neutron scattering diffraction, as reported in the literature [15].

The surfaces of the two sides of the as-quenched alloys show the characteristics of metallic glasses prepared by melt spinning methods (Fig. 3). The inner sides have small, parallel grooves due to the contact with the cooling wheel. The outer sides exhibit large randomly located hillocks.

The DSC traces of as-quenched glassy alloys are reported in Fig. 4 as function of temperature. The crystallization process occurs in two steps for the Ti-containing alloys, while the Zr-containing materials show only one peak in the DSC thermograms. The thermal stability increases with Cu concentration and the Zr-base alloys are more stable than the Ti-base.

A kinetic approach to the stability of amorphous alloys suggested that the crystallization temperature of a binary amorphous alloy $A_{1-x}B_x$ is controlled by the formation

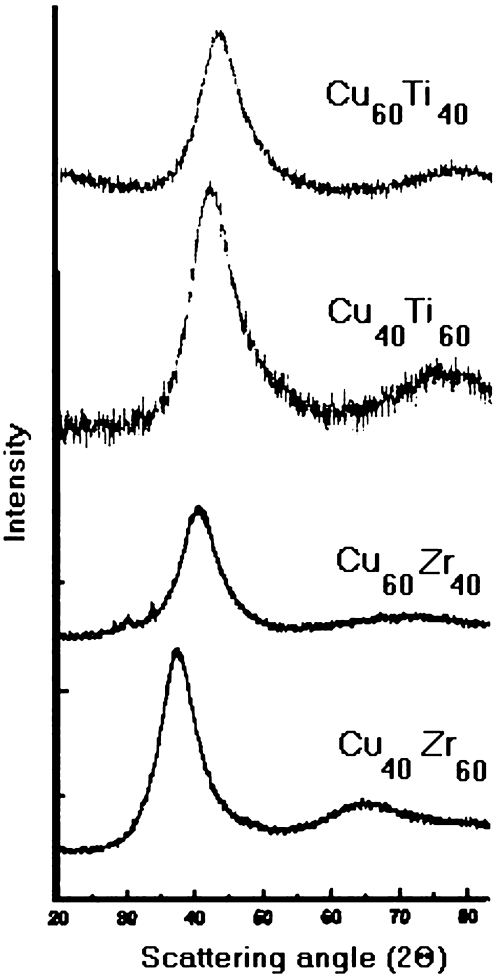

Fig. 1. X-ray diffraction pattern of as-quenched alloys.

enthalpy ΔH_h of a hole of the same size as the smallest atom B in the alloy [16]. With a semi-empirical model for monovacancies in metals and alloys an empirical linear correlation between T_x, the crystallization temperature, and ΔH_h for a large number of binary amorphous alloys has

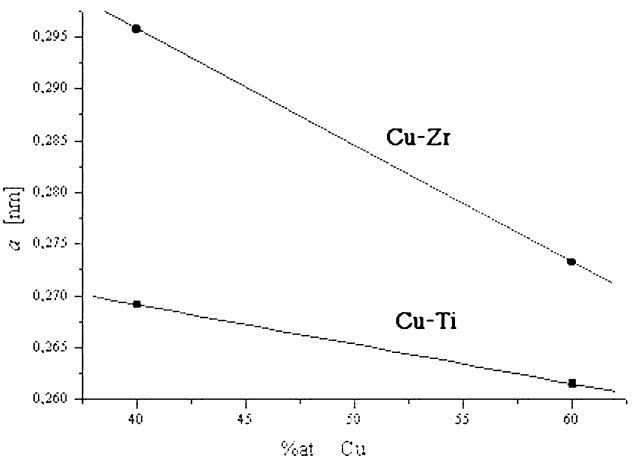

Fig. 2. Influence of Cu atomic concentration on the minimal distance *a*.

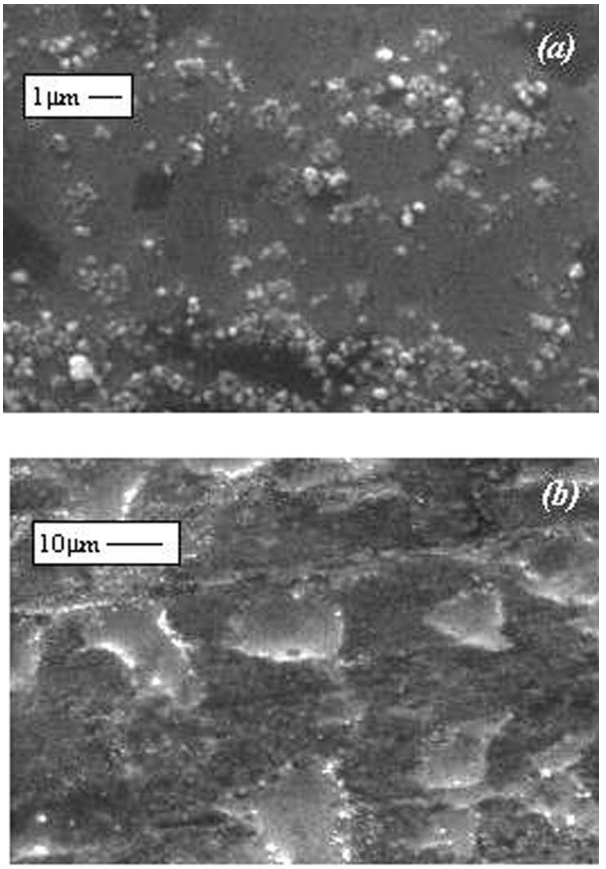

Fig. 3. SEM images of $Cu_{60}Zr_{40}$ amorphous alloy: (a) outer side and (b) inner side.

been determined [17]. The proportionality factor b is between 7 and 8. The value of ΔH_h is expressed as follows:

$$\Delta H_h^B = c\Delta H_A + (1-c)(V_B/V_A)^{5/6}\Delta H_B$$

where ΔH_A and ΔH_B are the formation enthalpies for a monovacancy in the pure metals, V_A and V_B are the molar volumes of the elements and c is the effective surface concentration expressed by means of:

$$c = xV_B^{2/3}[(1-x)V_A^{2/3} + xV_B^{2/3}]^{-1}$$

The formation enthalpy and the proportionality factor b for both as-quenched and HF treated alloys are reported in Table 1.

The effects of the HF activation treatment on the structures of the amorphous metals were investigated by XRD. The activation treatment in 1 M HF gives strong modification in the alloys. The samples become brittle and on the XRD patterns (Fig. 5) the Braggs peaks of Cu emerge from the amorphous halo. From line broadening analysis of Cu diffraction peaks, an average particle size of 7 nm has been estimated.

The crystallization process is strongly influenced by the activation treatment. An increase of the T_x and a decrease of total crystallization enthalpy for the Ti containing alloys are recorded (Fig. 6). The Zr containing alloys show a depletion in the total crystallization enthalpy and the DSC crystallization peaks appear broad and a shoulder on the crystallization peaks appears, especially in the $Cu_{60}Zr_{40}$ alloy. This shoulder can be attributed to nucleation and growth of a nanocrystalline phase induced by the HF treatment [16].

The surface modifications of HF treated alloys were investigated by SEM. The treatment with 0.1 M HF induces, on the sample surfaces, the formation of small crystals, especially on $Cu_{40}Zr_{60}$. The 1 M HF treatment causes a devitrification of the amorphous surfaces with the exposure of a great amount of copper particles, because Zr and Zr oxides dissolve more rapidly than Cu in HF and very porous surfaces are obtained (Fig. 7). The Ti containing alloys show a lower porosity than Zr alloys. In fact, the dissolution of Ti oxide layers, which cover the ribbon surfaces, are slower than Zr oxides (Fig. 8).

The results of the electrochemical tests for the as-quenched alloys in acid environment are reported in Fig. 9. The Tafel slope is ~120 mV for all samples. The alloys with high Cu content show higher exchange current density than both pure Cu and low Cu content alloys.

Moreover the $Cu_{60}Zr_{40}$ exhibits a exchange current density higher than $Cu_{60}Ti_{40}$. This is in agreement with the Brewer–Engle theory [1]. In fact, the activity of the Cu-valve metals alloys is higher than pure copper. It suggests electron transfer from copper to valve-metals resulting in d-band deficiency of the copper. This electronic interaction is higher in Cu–Zr than in Cu–Ti system, because the stability of internally paired non-bonding d-electrons, unavailable for bonding in pure metal, increases from 3d to 4d [18]. However, the low Cu content alloys show a lower activity than pure Cu, because the surface oxide layers are thick and the amount of active sites exposed is lower.

In an alkaline environment, the Zr oxides leach more markedly than the Ti oxides, so a higher amount of Cu is exposed to the solutions. It produces a marked difference in exchange current density between Zr and Ti containing alloys (Fig. 10). Moreover the exchange current densities of the alloys are higher in alkaline than in acid environment.

The 1 M HF activation treatment increases the electrocatalytic activity of the alloys (Fig. 11) with a higher Tafel slope than the as-quenched materials (~70 mV). These results are due to the valve metals dissolutions in HF, which induce a surface Cu enrichment and an increase of surface porosity, in agreement with SEM observations and XRD patterns.

However, in H_2SO_4 solution the cathodic polarization curves show an induction period that delays the beginning of the hydrogen evolution reaction. This is probably due to oxidation of Cu enriched surface in air, before the immersion in the reaction solution. This Cu oxide layer is partially dissolved by the acid, giving rise to the induction

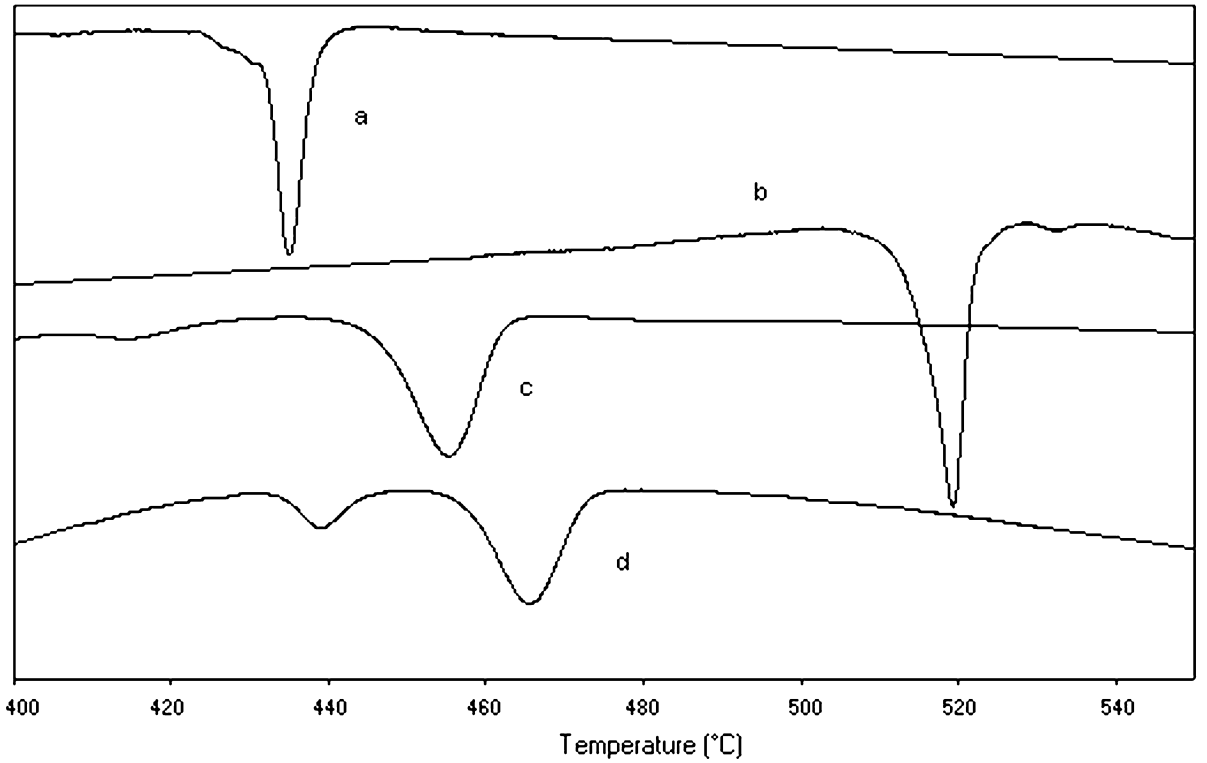

Fig. 4. DSC trace of as-quenched alloys: (a) $Cu_{40}Zr_{60}$; (b) $Cu_{60}Zr_{40}$; (c) $Cu_{40}Ti_{60}$; (d) $Cu_{60}Ti_{40}$.

time. In alkaline medium, the hydrogen evolution reaction starts at lower overvoltage, because the Cu oxide layer is stable in NaOH environments, and the exchange current density is higher than in H_2SO_4. After HF treatments, the low Cu content alloys show the highest electrocatalytic activity, because high surface porosity has been obtained by activation treatments. This is in agreement with DSC results. In fact the HF treated alloys with lower Cu content shift the T_x at higher values because more valve metals are dissolved.

The 0.1 M HF activation treatment produces an increase of activity although lower than the 1 M. However in acid environment, the catalysts exhibit no induction period, probably because this treatment produces a weaker structural change than the 1 M HF, but only the surface oxide layers are removed, as confirmed by SEM observation.

A galvanostatic experiment (14 h at 600 mA/cm^2) was performed on $Cu_{60}Ti_{40}$ and $Cu_{60}Zr_{40}$ as-quenched alloys to investigate the structural modification induced by H_2 adsorption. The DSC trace (Fig. 12) of Ti containing material shows an exothermic peak at ~150°C and a broad

Table 1
Hole formation enthalpy and proportional factor of investigated alloys

Alloy	ΔH_h(kJ/mol)	b (mol·K/kJ)
$Cu_{60}Zr_{40}$	95.50	8.24
$Cu_{40}Zr_{60}$	94.04	7.49
$Cu_{60}Ti_{40}$	99.00	7.37
$Cu_{40}Ti_{60}$	99.66	7.21
$Cu_{60}Zr_{40}$ HF treated	95.50	8.16
$Cu_{40}Zr_{60}$ HF treated	94.04	8.30
$Cu_{60}Ti_{40}$ HF treated	99.00	7.44
$Cu_{40}Ti_{60}$ HF treated	99.66	7.10

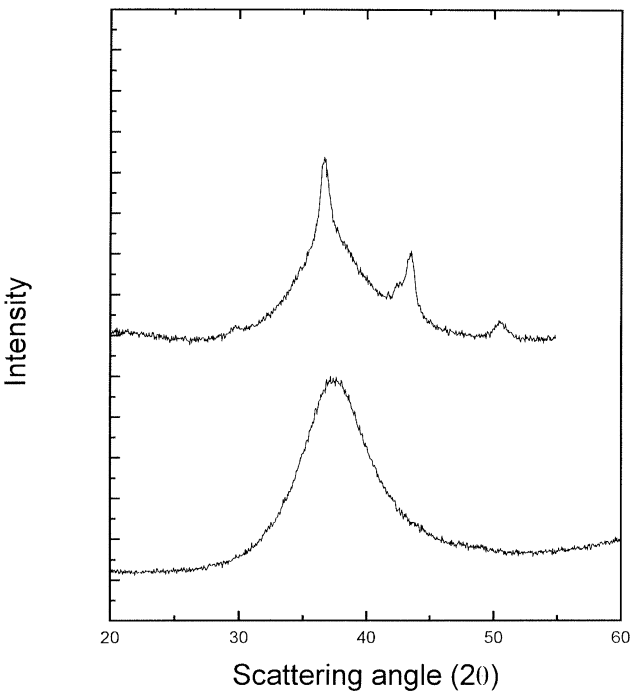

Fig. 5. XRD patterns of 1 M HF treated (upper) and as-quenched (lower) $Cu_{40}Zr_{60}$ alloy.

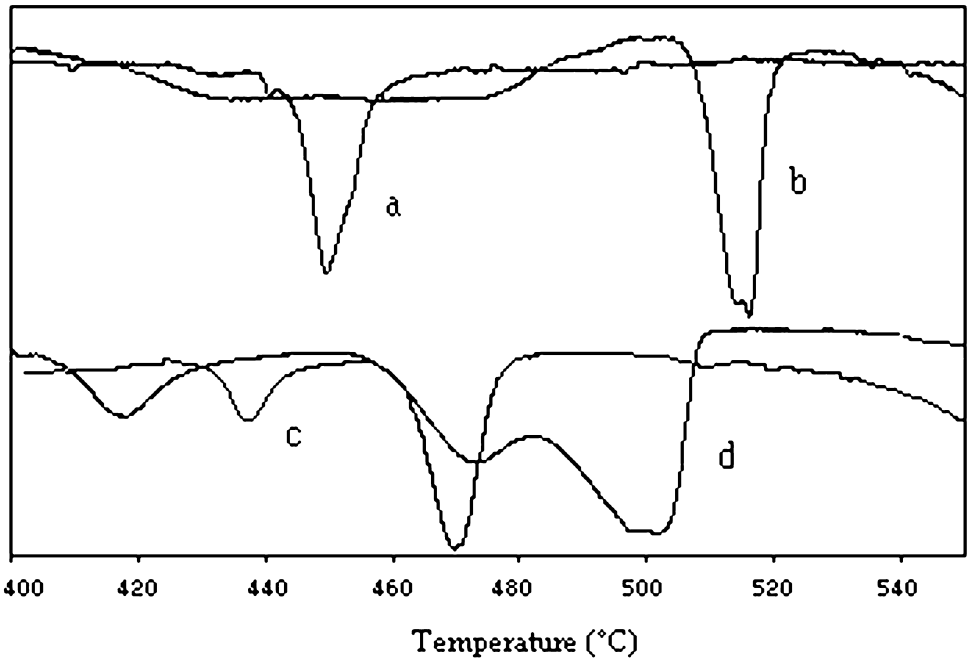

Fig. 6. DSC traces of 1 M HF treated alloys: (a) $Cu_{40}Zr_{60}$; (b) $Cu_{60}Zr_{40}$; (c) $Cu_{60}Ti_{40}$; (d) $Cu_{40}Ti_{60}$.

endothermic peak at ~400°C. These peaks are attributed to the formation of Cu and Ti hydride and to hydrogen desorption and consequently formation of γ-CuTi phase, respectively [19].

4. Conclusions

The amorphous Cu–Ti and Cu–Zr alloys after treatment with aqueous HF solutions have high electrocatalytic activity for the hydrogen evolution reaction in acid and especially in alkaline medium. This is caused firstly by the removal of inert films of Ti oxides and Zr oxides from the surfaces, and secondly by the porous layer of copper, which is stable, in alkaline environment, on the amorphous surfaces. Interesting results have been obtained by immersion in 0.1 M HF solutions, because the activity increases without strong structural and surface modifications of the catalysts.

Acknowledgements

The authors would like to acknowledge the MURST for the financial support of this work (Contract 9803113214_002, Project 'Alloys and Intermetallic Compounds: Thermodynamics, Physical Properties, Reactivity'), and Professor Baricco of University of Turin (Italy) for supplying amorphous alloys.

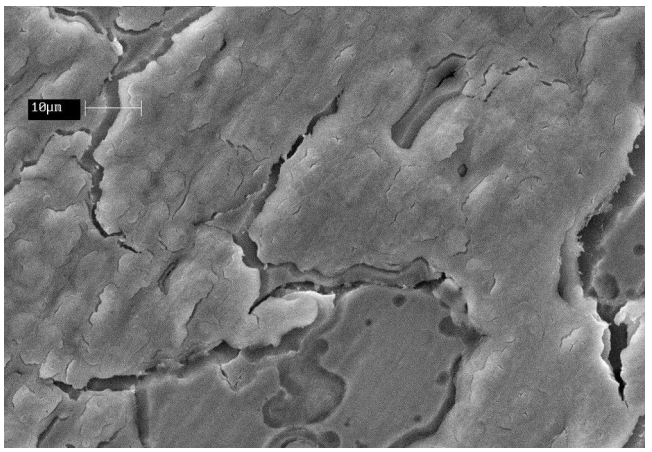

Fig. 7. SEM image of 1 M HF treated $Cu_{40}Zr_{60}$ surface.

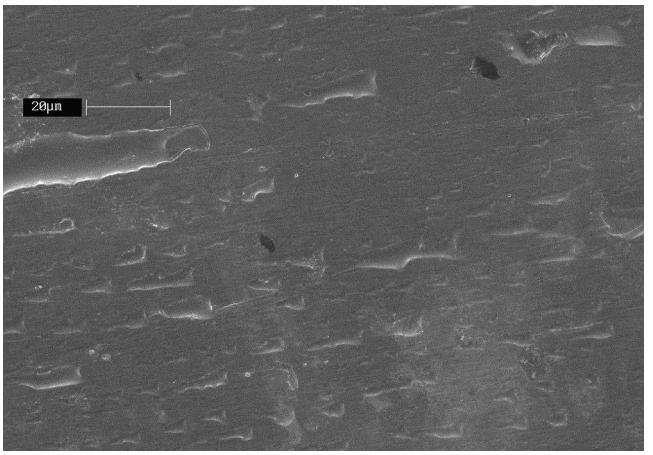

Fig. 8. SEM image of 1 M HF treated $Cu_{40}Ti_{60}$ surface.

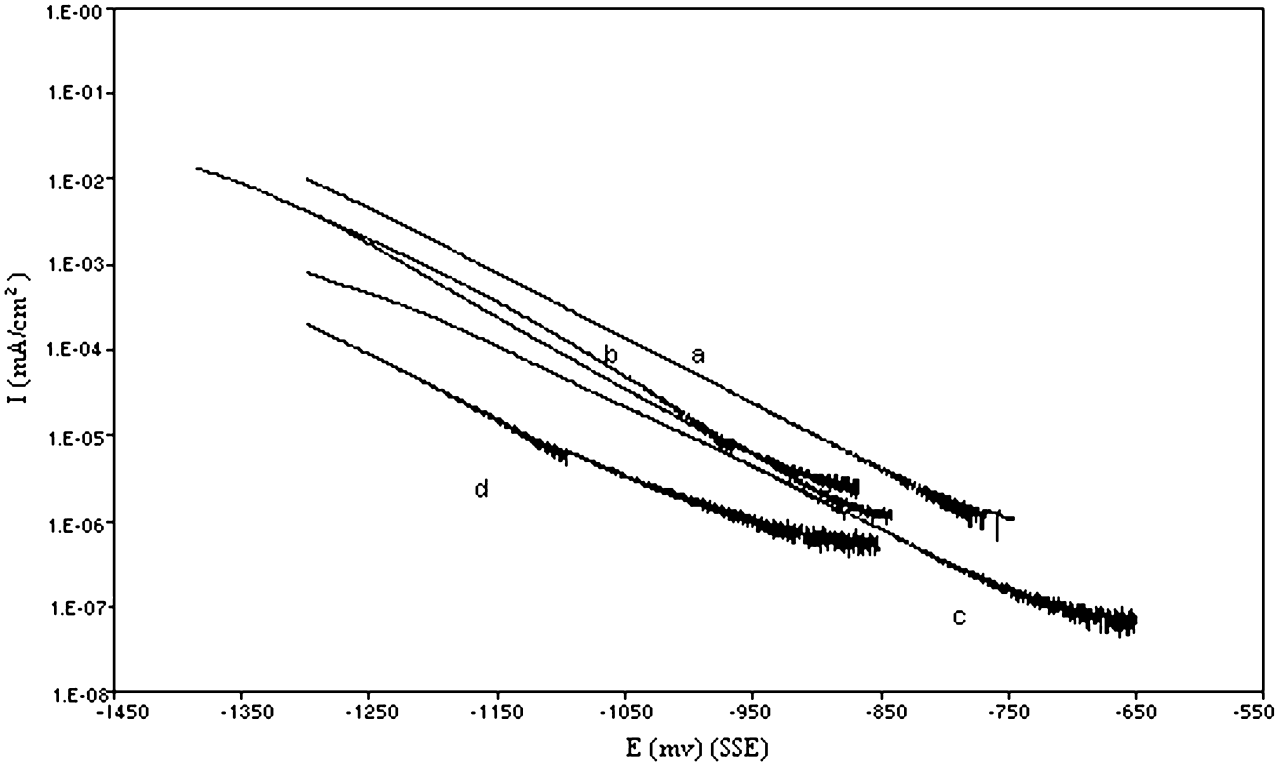

Fig. 9. Cathodic polarization curves in H_2SO_4 of amorphous as-quenched alloys: (a) $Cu_{60}Zr_{40}$; (b) $Cu_{60}Ti_{40}$; (c) $Cu_{40}Zr_{60}$; (d) $Cu_{40}Ti_{60}$. Cathodic polarization curves of pure Cu is the thickest.

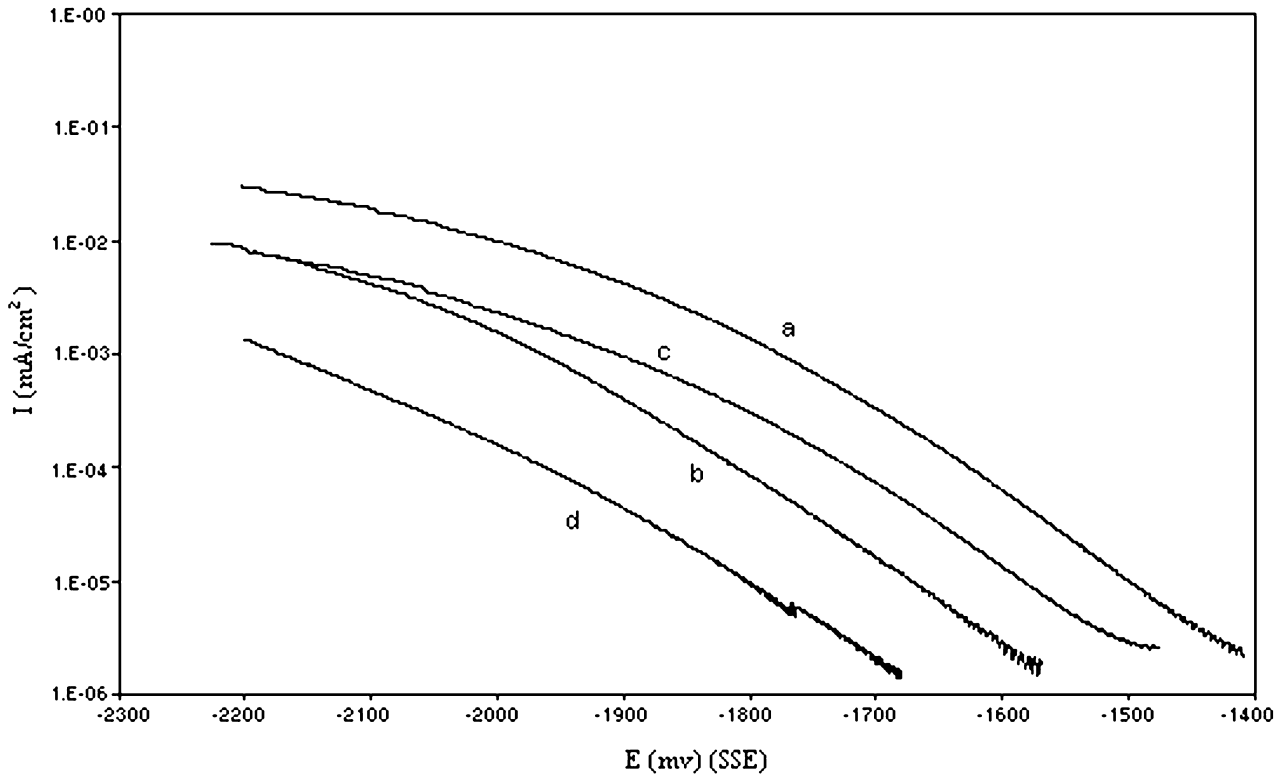

Fig. 10. Cathodic polarization curves in NaOH of amorphous as-quenched alloys: (a) $Cu_{60}Zr_{40}$; (b) $Cu_{60}Ti_{40}$; (c) $Cu_{40}Zr_{60}$; (d) $Cu_{40}Ti_{60}$.

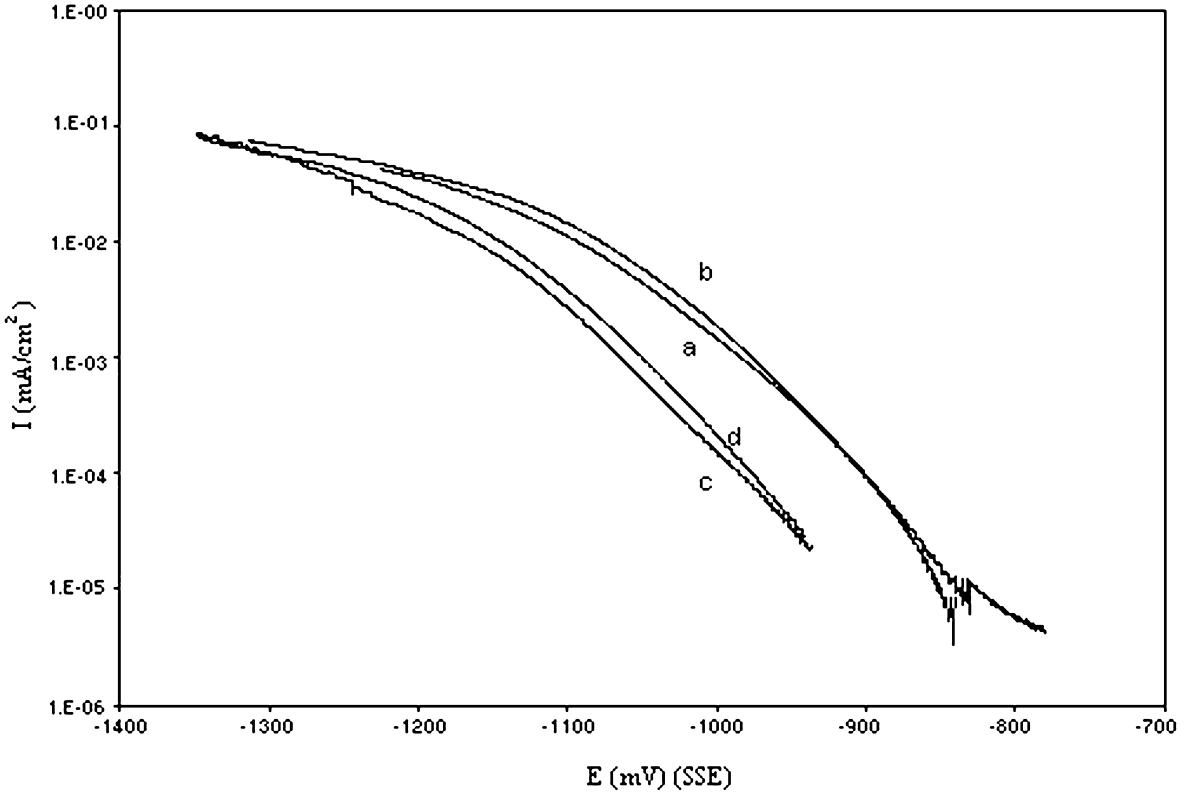

Fig. 11. Cathodic polarization curves in H_2SO_4 of 1 M HF treated alloys: (a) $Cu_{60}Zr_{40}$; (b) $Cu_{40}Zr_{60}$; (c) $Cu_{60}Ti_{40}$; (d) $Cu_{40}Ti_{60}$.

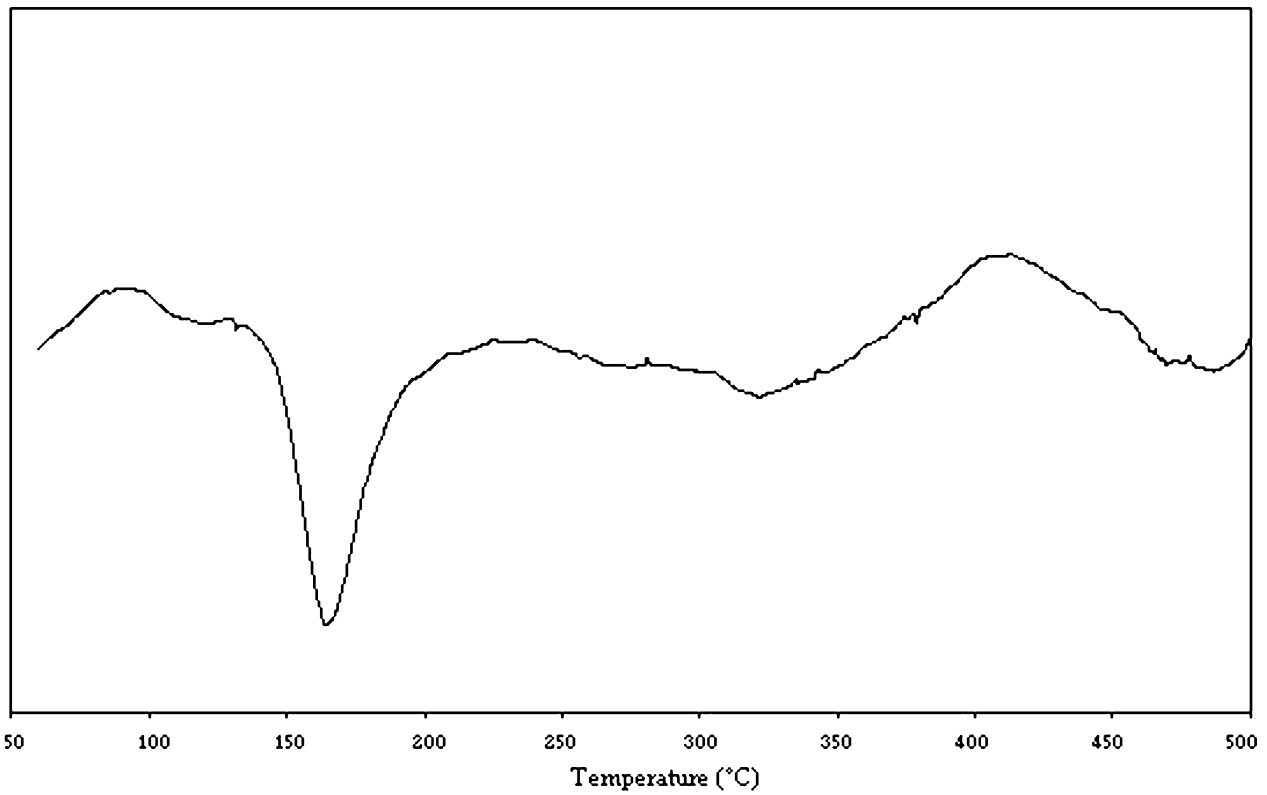

Fig. 12. DSC trace of as-quenched $Cu_{60}Ti_{40}$ after cathodic hydrogen charging for 14 h at 600 mA/cm^2.

References

[1] S. Trasatti, J. Electroanal. Chem. 39 (1972) 163.
[2] M.M. Jaksic, J. Mol. Catal. 38 (1986) 161.
[3] M. Hara, K. Asami, K. Hashimoto, T. Masumoto, Electrochim. Acta 25 (1980) 1091.
[4] A.J. Maeland, L.E. Tanner, G.G. Libowitz, J. Less-Common Met. 74 (1980) 279.
[5] M. Naka, K. Hashimoto, T. Masumoto, I. Okamoto, in: T. Masumoto, K. Suzuki (Eds.), Proceedings of the 4th International Conference On Rapidly Quenched Metals, Japanese Institute of Metals, Sendai, Japan, 1981, p. 1431.
[6] K. Machida, M. Enyo, I. Toyoshima, K. Miyahara, K. Kai, K. Suzuki, Bull. Chem. Soc. Jpn. 56 (1983) 3393.
[7] M. Enyo, T. Yamazaki, K. Kai, K. Suzuki, Electrochim. Acta 28 (1983) 1573.
[8] K. Machida, M. Enyo, K. Kai, K. Suzuki, J. Less-Common Met. 100 (1984) 377.
[9] K. Machida, M. Enyo, G. Adachi, J. Shiokawa, Electrochim. Acta 29 (1984) 807.
[10] G. Jorge, R. Faure, R. Durand, A.R. Yavari, Mat. Sci. Eng. 99 (1988) 517.
[11] A. Molnar, G.V. Smith, M. Bartok, Adv. Catal. 36 (1989) 329.
[12] S. Spriano, M. Baricco, C. Antonione, E. Angelini, F. Rosalbino, P. Spinelli, Electrochim. Acta 39 (1994) 1786.
[13] S. Enzo, R. Frattini, R. Gupta, P.P. Macri, G. Principi, L. Schiffini, G. Scipione, Acta Mater. 44 (1996) 3105.
[14] A. Guinier, in: H.M. Foley, M.A. Ruderman (Eds.), X-Ray Diffraction in Crystals, Imperfect Crystals and Amorphous Bodies, W.H. Freeman, San Francisco, 1963, p. 61.
[15] B. Grzeta, K. Dini, N. Cowlam, H.A. Davies, J. Phys. F: Met. Phys. 15 (1985) 2069.
[16] A.K. Bhatnagar, K.W. Rhie, D.G. Naugle, A. Wolfenden, B.H. Zhang, T.O. Callaway, W.D. Bruton, C.R. Hu, J. Phys. Condens. Matter. 2 (1990) 2625.
[17] R.A. Miedema, Z. Metallk. 70 (1979) 345.
[18] C. Brewer, in: M.C. Keefe, A. Navrotski (Eds.), Structure and Bonding in Crystals, Vol. 1, Academic Press, New York, 1981, p. 155.
[19] B. Rodmacq, A. Chamberod, Phys. Rev. B 38 (1988) 1116.